



MOCVD Growth and Characterization of Cobalt Phosphide Thin Films on InP Substrates

Davide Barreca,^{a,*} Andrea Camporese,^b Maurizio Casarin,^c Naida El Habra,^b Andrea Gasparotto,^d Marco Natali,^{b,z} Gilberto Rossetto,^b Eugenio Tondello,^c and Pierino Zanella^b

^aISTM—CNR, Sezione di Padova and INSTM, Dipartimento CIMA, University of Padova, I-35131 Padova, Italy

^bICIS—CNR, I-35127 Padova, Italy

^cDipartimento CIMA, University of Padova and INSTM, I-35131 Padova, Italy

^dDipartimento di Fisica “G. Galilei”, Istituto Nazionale Fisica della Materia (INFM), I-35131 Padova, Italy

Cobalt phosphide thin films were grown by metal-organic chemical vapor deposition (MOCVD) in H₂ atmospheres on InP(001) substrates using bis(η-methylcyclopentadienyl)Co(II) [Co(Cp^{Me})₂] and phosphine (PH₃) precursors at 550°C. Film microstructure, composition, and morphology were investigated in detail by X-ray diffraction, X-ray photoelectron spectroscopy (XPS), Rutherford backscattering (RBS), and atomic force microscopy. Films were crystalline and consisted mainly of the orthorhombic CoP phase and some amount of the CoP₂ phase. XPS measurements indicate an oxidation state (III) for Co, while the P/Co ratio was found by RBS to lie in the range 1–2. The coatings were highly textured with (202), (103) CoP, and (−311) CoP₂ crystal planes parallel to the substrate surface. The root mean square surface roughness was below 10 Å for thicknesses smaller than 20 nm and increased to a maximum of 70 Å for a 35 nm thick film. Cobalt and In intermixing was investigated by XPS depth profiles. © 2004 The Electrochemical Society. [DOI: 10.1149/1.1782633] All rights reserved.

Manuscript submitted September 8, 2003; revised manuscript received February 25, 2004. Available electronically August 18, 2004.

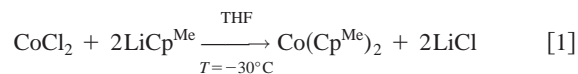
A great deal of attention has been recently devoted to a new class of electronic devices known as spintronic devices, that involve manipulation of both the electron spin and charge.^{1,2} This widespread interest is mainly related to the possibility of fabricating nonvolatile magnetic random access memories (MRAM). Current MRAM devices are based on the giant magnetoresistance effect (GMR), which occurs in metal multilayer systems where a nonferromagnetic layer is sandwiched between two ferromagnetic ones (*e.g.*, Co/Cu/Co). As the magnetization of the Co layers changes from parallel to antiparallel alignment, the multilayer resistance can increase by as much as 20%.^{1,2} While prototype MRAM devices have already been developed, significant technological problems still remain to be solved, in particular concerning the integration of ferromagnetic materials with semiconductor electronics. In this context, the search for alternative ferromagnetic materials is a major concern. Currently the most promising materials appear to be diluted magnetic semiconductors (DMS), such as MnGaAs^{3,4} and MnCdGeP₂,⁵ and digital alloys, that consist of alternating ultrathin layers of semiconductors (*e.g.*, GaAs, GaSb), and ferromagnetic compounds (*e.g.*, MnAs, MnSb).^{6–8} While DMS growth has been performed almost exclusively by low-temperature molecular beam epitaxy (MBE), in order to avoid phase segregation, the growth of metal-pnictide compounds such as MnAs, MnSb, or CoP appears possible also by metallorganic chemical vapor deposition (MOCVD), as proven by recent works regarding CoP deposition on Si.⁹

This paper reports on the MOCVD growth and characterization of cobalt-phosphide thin films on InP(001) substrates with the aim to obtain epitaxial film deposition. Cobalt phosphide thin films were grown on InP(001) in H₂ atmospheres using Co(Cp^{Me})₂ (Cp^{Me} = methylcyclopentadiene) and PH₃ as Co and P precursors, respectively, and subsequently were characterized by different analytical techniques to attain an insight on their chemical-physical characteristics and the dependence of these on the synthesis conditions.

Experimental

Precursor synthesis and characterization.—The cobalt precursor synthesis was carried out in a glove box filled with purified nitrogen to avoid its decomposition. All solvents were dried according to already established procedures.¹⁰ The bis(η⁵-methylcyclopenta-

dienyl)Co(II) [Co(Cp^{Me})₂, Cp^{Me} = −C₅H₄CH₃] was obtained by the reaction of methylcyclopentadienyl lithium (LiCp^{Me}) with anhydrous cobalt dichloride in (1:2 stoichiometric ratio) tetrahydrofuran (THF) solution



A solution in THF of the anhydrous cobalt dichloride was slowly added at low temperature ($T = -30^\circ\text{C}$) to a stirred solution of LiCp^{Me} in THF. The solution immediately assumed a dark color. After 2 h cooling was stopped, and the solution was allowed to reach room temperature and kept under stirring overnight. The THF solvent was evaporated under vacuum. Cyclohexane was added to the reaction mixture and the obtained suspension was filtered to eliminate LiCl. The solvent of the clear solution was evaporated under vacuum and the obtained glassy product (almost black, yield = 78.6%) was purified by sublimation at $T = 35^\circ\text{C}$ and $p = 0.02$ Torr and characterized by ¹H-NMR, with good agreement with previous data.¹¹ Compared to CoCp₂, that is a commercially available Co precursor, we found that Co(Cp^{Me})₂ is slightly more volatile [we found that Co(Cp^{Me})₂ sublimed readily at a pressure of 10^{−2} Torr at 35°C, while CoCp₂ sublimed readily at a pressure of 10^{−4} Torr at 40°C] thereby facilitating MOCVD growth.

MOCVD growth was performed with a low pressure Aixtron AIX200 reactor at a total pressure of 20 mbar and a growth temperature of 550°C. The precursors for Co and P were Co(Cp^{Me})₂ and PH₃, respectively. Co(Cp^{Me})₂ was dispersed in glass beads, loaded into a bubbler at 35°C, and transported into the reaction chamber by Pd-purified H₂ carrier gas, acting also as a reducing atmosphere. A series of specimens was grown at constant PH₃ flow rate of 300 sccm and different H₂ flow rates (50, 100, 300 sccm) through a Co bubbler for 1 h (samples A, B, C) and at a constant flow rate (300 sccm) with different growth time 30 min, 1 h, 2 h (samples D, C, E). Substrates were Fe-doped semi-insulating, epitaxially InP(001) wafers from Crismatec. All the obtained films appeared homogeneous and mirror-like to the eye.

X-ray diffraction (XRD) spectra were recorded with a Philips PW1830 powder diffractometer in Bragg-Brentano geometry using Ni filtered Cu Kα (40 kV, 30 mA) radiation. The detector was a Xe gas proportional counter equipped with a secondary curved graphite

* Electrochemical Society Active Member.

^z E-mail: natali@icis.cnr.it

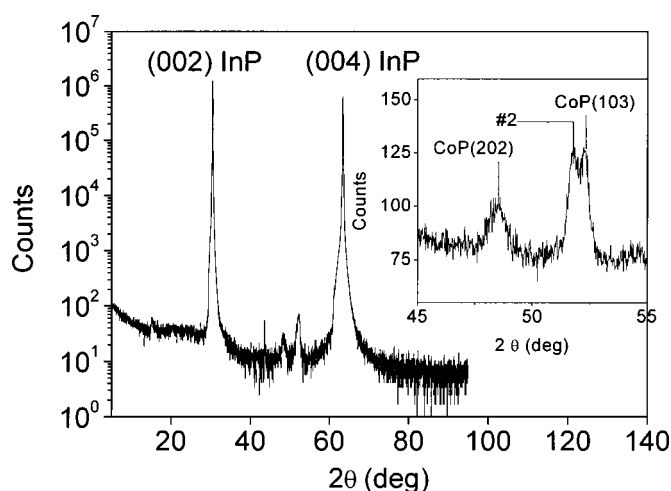


Figure 1. XRD spectrum of sample E (31 nm thickness). The InP(002) and InP(004) substrate peaks are observed as well as three film peaks, shown in the inset.

monochromator. Peak positions were determined with a statistical error of $\delta(2\theta) = 0.02^\circ$. Reflectivity measurements to determine film thickness were performed using a Philips MRD high resolution diffractometer with monochromatized Cu K α radiation. A Bartels monochromator was used, consisting of four germanium crystals reflecting from the (220) planes, producing a beam divergence of 12 arcsec and a wavelength spread $\Delta\lambda/\lambda = 10^{-5}$.

X-ray photoelectron spectroscopy (XPS) measurements were performed by a Perkin-Elmer Φ 5600ci spectrometer using monochromatized Al K α radiation (1486.6 eV). The working pressure was less than $2 \cdot 10^{-9}$ mbar. The spectrometer was calibrated by assuming the binding energy (BE) of the Au 4f $_{7/2}$ line at 83.9 eV with respect to the Fermi level. The standard deviation for the BE values was ± 0.2 eV. The reported BE were corrected for the charging effects, assigning to the C 1s line of adventitious carbon the BE value of 284.8 eV.¹² Survey scans were obtained in the 0-1350 eV range. Detailed scans were recorded for the O 1s, C 1s, P 2p, Co 2p, Co LMM, In 3d. The atomic composition was evaluated using sensitivity factors supplied by Perkin-Elmer. Depth profiles were carried out by Ar $^+$ sputtering at 2.5 keV with an argon partial pressure of $5 \cdot 10^{-8}$ mbar. The depth of the XPS craters was measured by means of a Tencor Alpha Step profiler. Film thickness was determined from the XPS profiles assuming the interface lies at the point where Co drops to 50% of its maximum value.

Rutherford back scattering (RBS) measurements were performed at Laboratori Nazionali Legnaro, Italy, using the 7 MV Van de Graaf CN accelerator, with a 2.2 MeV He $^+$ beam.

Atomic force microscopy (AFM, Park CP model) was performed to analyze surface morphology in the contact mode using a Ultra-lever $^{\text{TM}}$ silicon cantilever tip with a nominal radius of 10 nm. Surface roughness was determined as root-mean-square (rms) values from several $2 \times 2 \mu\text{m}^2$ micrographs.

Electrical resistivity measurements were performed in the Van der Pauw geometry using indium contacts and a four-point probe. The resistivity was calculated from the measured resistance and the layer thickness according to the formula from Ref. 13.

Results and Discussion

The cobalt phosphide film growth rate ranged from 0.1 to 0.33 nm/min, increasing with the H $_2$ carrier gas flow through the Co(Cp $^{\text{Me}}$) $_2$ bubbler. The low growth rates are primarily due to the relatively low volatility of the precursor and to some extent to the long gas transport lines (about 1.5 m) of the reactor used. A typical $\theta/2\theta$ scan XRD spectrum is shown in Fig. 1. Intense substrate peaks are observed at $2\theta = 30.45^\circ$ and $2\theta = 63.31^\circ$ corresponding to

InP(002) and InP(004) Bragg reflections, respectively. Three weak film peaks are observed at $2\theta_1 = 48.47^\circ$, $2\theta_2 = 51.79^\circ$ and $2\theta_3 = 52.22^\circ$, respectively. We assign the first and third peak mentioned to the CoP(202) and CoP(103) Bragg reflections, that according to the JCPDS powder diffraction database occur at $2\theta = 48.404^\circ$ and $2\theta = 52.294^\circ$, respectively (JCPDS no. 29-497). The second peak could not be unambiguously identified. Possible assignments include cubic Co(002) $2\theta = 51.524^\circ$ (JCPDS no. 15-806), Co $_2$ P(131) $2\theta = 51.549^\circ$, Co $_2$ P(002) $2\theta = 52.031^\circ$ (JCPDS no. 32-0306), CoP $_2$ (-113) $2\theta = 51.599^\circ$ and CoP $_2$ (-311) $2\theta = 51.946^\circ$ (JCPDS no. 26-481). The reflection lying closest to the observed peak is CoP $_2$ (-311), but the discrepancy is still 0.15°. A similar situation was observed for all the other grown samples, suggesting that the films are crystalline and mainly constituted of the CoP phase and possibly a CoP $_2$ phase. The peaks near 18° and 44° were not observed systematically and do not correspond to any of the known cobalt phosphide phases. We therefore attribute them to contaminations due to sample handling.

All the film peaks showed a strong preferential alignment of their Bragg planes parallel to the substrate surface (3° mosaic spread), as established by rocking-curve measurements, keeping the detector fixed at the Bragg angle and rotating the sample Ω angle. A further support for this conclusion comes from the absence of any other reflections from CoP and CoP $_2$, that should have been observed in the case of randomly oriented grains. Moreover no film reflections from Bragg planes inclined with respect to the surface were observed by recording 2θ scans for different sample (incidence) angles Ω , while simultaneously spinning the sample about its surface normal. We were thus not able to establish from the XRD measurements whether the films are epitaxial.

From the CoP(202) film peak width a crystallite size was determined that ranged from 3 nm for the thinnest films (4 ± 1 nm thickness) to 6 nm for the thickest films (31 ± 2 nm thickness). This crystallite size corresponds to a coherence length of CoP grains along the [202] direction, that in our case lies perpendicular to the surface.

Figure 2a shows a typical AFM micrograph of the film surface morphology. Grains of average in-plane diameter ≈ 80 nm are observed for all samples. The surface roughness is plotted as a function of film thickness in Fig. 2b and shows a plateau region for film thickness below 20 nm, where the film roughness is lower than 10 Å. For larger thicknesses the roughness increases rapidly, reaching a maximum of 70 Å for a 35 nm thick film, corresponding to 20% of the thickness. Moreover the film surface roughness was found to increase with the H $_2$ flow rate through the Co bubbler and with deposition time (not shown).

Surface and in-depth film composition of the films were investigated by XPS analysis. Irrespective of the synthesis conditions, a qualitatively similar surface composition was observed for all samples. Wide scan surface spectra (Fig. 3) displayed signals arising from Co, P, C, and O. In particular, the Co 2p region showed a position [BE(Co2p $_{3/2}$) = 779.6 eV, (fwhm) ≈ 1.7 eV] and a band-shape very similar to those reported for both Co $_2$ P and CoP.¹⁴ The presence of Co(II) was excluded, since its characteristic shake-up peaks at ≈ 5.4 eV from the principal spin-orbit components were not observed.^{15,16}

Despite the presence of oxygen, the formation of cobalt oxides could be unambiguously ruled out on the basis of BEs and Auger parameter values.^{17,18} In particular, Auger parameter values, calculated as the sum of Co 2p $_{3/2}$ BE, and Co LMM kinetic energy (KE)¹² varied between 1551.5 and 1551.9 eV. Indeed, oxygen presence could be related to the surface oxidation of cobalt phosphides to phosphates. As a matter of fact, P 2p surface photopeak (Fig. 3, inset) always showed two distinct components. The major one (BE ≈ 129.7 eV, fwhm ≈ 2.0 eV, $\approx 80\%$) was ascribed to P in phosphides,^{14,17} while the second (BE ≈ 133.7 eV, fwhm ≈ 2.6 eV, $\approx 20\%$) was related to the presence of phosphates.¹⁷ The latter component was always reduced to noise level after a mild Ar $^+$ erosion,

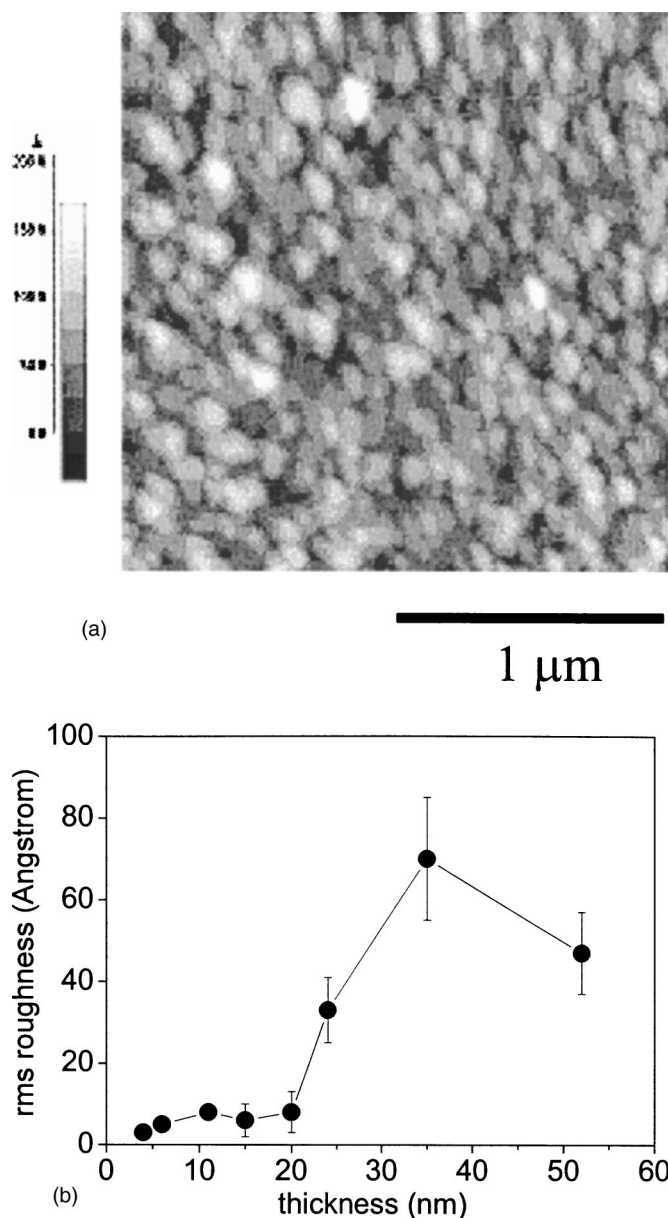


Figure 2. (a, top) Representative AFM image of sample E ($2 \times 2 \mu\text{m}^2$ area, the grayscale extends over 200 Å in depth); (b, bottom) rms roughness as a function of film thickness.

confirming that phosphate presence was merely limited to the outermost sample layers. Nevertheless, this phenomenon prevented the unambiguous identification of the Co-P phase by an estimation of P/Co surface atomic ratio.

In order to attain a deeper insight into film composition, with particular attention to the Co-P relative amounts, XPS depth profiling was performed on different specimens. As a general rule, carbon signals disappeared after a mild sputtering, indicating that the presence of C arose mainly from atmospheric contamination and that the Co precursor underwent a clean conversion into Co phosphides under the adopted synthetic conditions. A representative depth profile is displayed in Fig. 4.

The most striking feature regards the wideness of the film-substrate interface. A decrease of the Co atomic percentage is observed as a function of depth, that is accompanied by a corresponding increase of the In atomic percentage. Conversely, the P percentage remains almost constant from the surface to the inner sample layers. In order to investigate the eventual presence of P

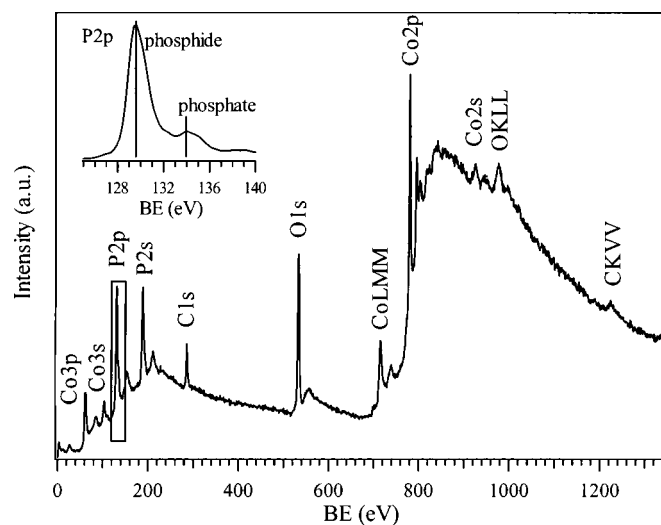


Figure 3. Surface XPS wide scan spectrum of cobalt phosphide film with 31 ± 2 nm thickness. The inset displays the P 2p photopeak, showing the phosphide and phosphate components.

preferential sputtering,¹² further erosion experiments were carried out in the same conditions on bare InP substrates, with or without annealing in air at 550°C (the growth temperature of cobalt phosphide films). The obtained results showed that the In/P atomic ratio was close to the stoichiometric value (≈ 1) on the sample surface, but almost doubled after a mild Ar^+ sputtering. On this basis, we suggest that a similar P behavior might occur during depth profiling of cobalt phosphide thin films. In this case, the real P/Co atomic ratio in the first 20 nm would be close to 1, suggesting the presence of CoP as the main phase in this region. Nevertheless, a more detailed phase identification is also prevented because of the appreciable film-substrate intermixing. Therefore the already mentioned estimate of the P/Co atomic ratio needs to be taken with great caution.

To obtain additional information on film stoichiometry we performed Rutherford backscattering (RBS) measurements. We analyzed the spectra in a first attempt by assuming homogeneous films that do not contain any In atoms. In this case the P/Co atomic ratio close to 2 was found for most films. However as the XPS measurements have shown significant film-substrate intermixing is occurring and In atoms are present over a considerable fraction of the film

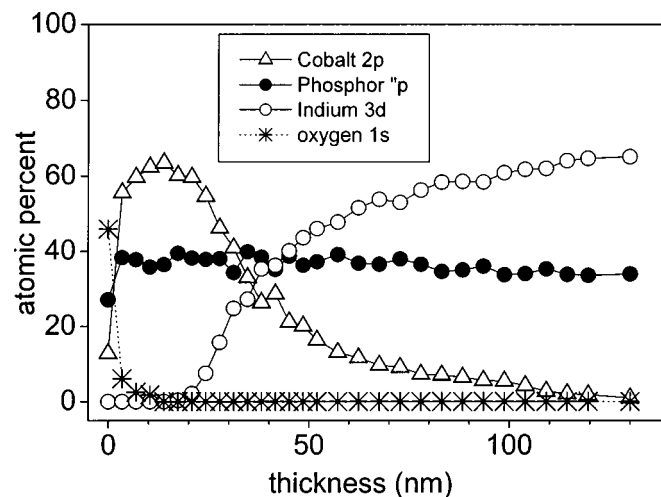


Figure 4. XPS depth profile of cobalt phosphide film with 31 ± 2 nm thickness.

thickness. We here note that the Rutherford cross section of In is much higher than that of Co [the ratio of the cross sections is given in terms of the atomic numbers of In and Co by $(Z_{\text{In}}/Z_{\text{Co}})^2 = (49/27)^2 \approx 3.3$]. As a consequence very small uncertainties of the In concentration in the film can give rise to large uncertainties in the Co concentration. To obtain meaningful P/Co atomic ratios the RBS spectra should then be simulated with appropriate In diffusion profiles. This, however, was not possible due to the small thickness of the films (<52 nm), that made it impossible to discriminate between a constant In concentration or a In diffusion profile. The only conclusion that we could draw from the RBS measurements was that the P/Co atomic ratio is in the range of 1-2. This seems to be in qualitative agreement with the XRD measurements that indicate the presence of some amount of CoP_2 phase, besides the CoP phase.

The resistivity of the samples was between 0.02 and 0.08 Ω cm, the minimum occurring at 15 nm thickness and the maximum at 4 nm thickness. For film thicknesses between 15 and 31 nm a gradual increase of resistivity from 0.020 ± 0.002 to 0.030 ± 0.002 Ω cm occurred, that may be related to the rapidly increasing surface roughness for these films. On the other hand the decrease of resistivity between 4 and 15 nm is probably due to the presence of insulating phosphate in the outer layers, that accounts for a larger material fraction in thinner films. The resistivity values found are somewhat higher than those reported in Ref. 9, i.e., $4.5 \cdot 10^{-4}$ – 10^{-3} Ω cm. We do not understand the reason for the higher resistivity values determined by us, however, we believe that these differences are related to the different structures of the films, that in our case were composed out of crystalline CoP and CoP_2 phases, while films reported in Ref. 9 were partly amorphous and partly crystalline CoP.

Conclusions

Cobalt phosphide thin films were grown by MOCVD on InP(001) substrates in H_2 atmospheres, at a substrate temperature of 550°C. The films were highly oriented, with CoP(202), CoP(103), and $\text{CoP}_2(-311)$ crystal planes parallel to the substrate surface. Film stoichiometry was difficult to evaluate by XPS due to prefer-

ential sputtering of P during Ar ion erosion and in RBS due to film-substrate intermixing. Nevertheless a P/Co ratio was estimated lying in the range of 1-2. Surface roughness was found to increase with H_2 flow rate, deposition time and film thickness, with an abrupt increase of roughness above 20 nm. The film resistivity was of the order 0.02-0.08 Ω cm and dependent on the film thickness, probably correlated with the surface morphology.

Acknowledgments

The authors thank Dr. G. Salmaso and V. Rigato from INFN, Legnaro, Italy, for performing RBS measurements.

ICIS-CNR assisted in meeting the publication costs of this article.

References

1. G. Prinz, *Science*, **282**, 1660 (1998).
2. S. A. Wolf, D. D. Awschalom, R. A. Buhrman, J. M. Daughton, S. von Molnar, M. L. Roukes, A. Y. Chitchekanova, and D. M. Treger, *Science*, **294**, 1488 (2001).
3. H. Ohno, *Science*, **281**, 951 (1998).
4. M. Henini, *III-V Rev.*, **13**, 32 (2000).
5. G. A. Medvedkin, T. Ishibashi, T. Nishi, K. Hayata, Y. Hasegawa, and K. Sato, *Jpn. J. Appl. Phys., Part 2*, **39**, L949 (2000).
6. R. K. Kawakami, E. Johnston-Halperin, L. F. Chen, M. Hanson, N. Guebel, J. S. Speck, A. C. Gossard, and A. A. Awschalom, *Appl. Phys. Lett.*, **77**, 2379 (2000).
7. F. Matsukara, E. Abe, and H. Ohno, *J. Appl. Phys.*, **87**, 6442 (2000).
8. M. Tanaka and K. Takahashi, *J. Cryst. Growth*, **227-228**, 847 (2001).
9. Y. Senzaki and W. Gladfelter, *Polyhedron*, **13**, 1159 (1994).
10. J. M. Marsella and K. G. Caulton, *J. Am. Chem. Soc.*, **14**, 2361 (1982).
11. M. F. Rettig and R. S. Drago, *J. Am. Chem. Soc.*, **91**, 1361 (1969).
12. D. Briggs and M. P. Seah, in *Practical Surface Analysis*, Vol. 1, John Wiley & Sons, New York (1990).
13. L. J. Van der Pauw, *Philips Tech. Rev.*, **20**, 220 (1959).
14. V. V. Nemoshkalenko, V. V. Didyk, V. P. Krivitskii, and A. I. Senkevich, *Russ. J. Inorg. Chem.*, **28**, 1239 (1983).
15. V. M. Jimenez, J. P. Espinos, and A. R. Gonzalez-Elipe, *Surf. Interface Anal.*, **26**, 62 (1998).
16. L. Armelao, D. Barreca, S. Gross, A. Martucci, M. Tieto, and E. Tondello, *J. Non-Cryst. Solids*, **477**, 293 (2001).
17. J. F. Moulder, W. F. Stickle, P. E. Sobol, and K. D. Bomben, in *Handbook of X-Ray Photoelectron Spectroscopy*, Perkin-Elmer Corporation, Eden Prairie, MN (1992).
18. D. Barreca, C. Massignan, S. Daolio, M. Fabrizio, C. Piccirillo, L. Armelao, and E. Tondello, *Chem. Mater.*, **13**, 588 (2001).